Trends in the potential distribution of mangroves in the Eastern Pacific under climate change scenarios

Patricia González-Zamorano

zamorano04@cibnor.mx

Centro de Investigaciones Biológicas del Noroeste

Felipe Andrés Toro-Cardona

Universidad de Antioquía

Joaquín Rivera Rosas

Centro de Investigaciones Biológicas del Noroeste

Salvador Emilio Lluch-Cota

Centro de Investigaciones Biológicas del Noroeste

David Arturo Paz-García

Centro de Investigaciones Biológicas del Noroeste

Article

Keywords: Conservation, Ecological niche modeling, Topographic constraints, Climate refugia, Habitat loss, Coastal ecosystems

Posted Date: June 19th, 2026

DOI: https://doi.org/10.21203/rs.3.rs-9986630/v1

Additional Declarations: No competing interests reported.

Abstract

Mangroves provide key coastal ecosystem services but are highly vulnerable to climate change. Their future responses remain uncertain in regions with strong topographic constraints, such as the Eastern Pacific, characterized by fragmented low-elevation coastal areas and biogeographic isolation. We assessed potential distribution trends of three dominant mangrove species (*Avicennia germinans*, *Laguncularia racemosa*, and *Rhizophora mangle*) across provinces and ecoregions under six CMIP6 climate scenarios by integrating topographic constraints as spatial filters of effective habitat availability, retained only 18.9% of climate-only projected areas. Models projected stable latitudinal limits from southern California to northern Peru, indicating that future changes will occur within the current range rather than through poleward expansion. Contraction trends were concentrated in tropical sectors, whereas potential inland expansion was associated with low-elevation coastal areas near latitudinal margins. Spatial responses were strongly asymmetric: the Tropical Eastern Pacific showed persistent loss trends, whereas the Warm Temperate Northeast Pacific exhibited stability–gain patterns linked with low-elevation coastal plains. The Galápagos Province remained highly stable across scenarios. Species responses differed: *R. mangle* showed the greatest losses, *A. germinans* the highest stability, and *L. racemosa* intermediate trends. Overall, projected mangrove distribution in the Eastern Pacific depends on the interaction between climate and topographically constrained habitats, highlighting the importance of conserving low-elevation coastal areas that facilitate inland migration under climate change.

Introduction

Mangrove forests are among the most productive coastal ecosystems, providing a wide range of ecosystem services, including coastal protection, carbon sequestration, fisheries support, and nutrient cycling [1]. Despite their ecological and socio-economic importance, global mangrove extent has declined by approximately 4.5% over the last 25 years due to human activities and degradation [2, 3].

Climate change is a key driver of mangrove distribution, structure, and biomass. The projected increases in temperature (2.7–3.2°C) and sea level rise (0.5–0.9 m) by the end of the century, along with more frequent extreme events, are expected to alter mangrove structure, function, and distribution [4, 5, 6]. Mangrove species are particularly sensitive to changes in temperature, precipitation, and sea level, making them highly vulnerable to future climatic shifts [7, 8]. Projections indicate a 10 to 15% decline in global mangrove coverage by the end of the century [9]. These changes may reduce ecosystem services and increase vulnerability in densely populated coastal regions [10, 11]. Global projections indicate substantial declines in mangrove coverage and consistent spatial trends characterized by poleward expansion in temperate regions and contraction in tropical zones [12, 13]. However, regional studies reveal contrasting responses associated with local climatic and environmental conditions [14, 15, 16, 17]. These discrepancies highlight the importance of regional assessments for evaluating spatially heterogeneous coastal responses and supporting conservation and climate adaptation strategies [18, 19, 20].

The Eastern Pacific remains understudied in mangrove climate projections. Global studies project contrasting trends among provinces, including potential increases associated with northward expansion [13], whereas regional evidence indicates stable northern limits constrained by ocean circulation and dispersal barriers such as Punta Eugenia, Mexico [15, 17, 21]. In tropical sectors of the Eastern Pacific, regional assessments remain limited despite projections of substantial losses [13].

The region corresponds to a tectonically active coastal margin characterized by narrow continental shelves, fragmented low-elevation coastal areas, and abrupt relief [22, 23]. Under these conditions, mangrove persistence and inland migration depend not only on climatic conditions but also on the availability of effective habitat constrained by topography. Additionally, historical isolation associated with the Eastern Pacific Barrier has contributed to relatively low species richness and genetic diversity, potentially limiting adaptive capacity under climate change [24, 25].

Previous mangrove distribution models under climate change have incorporated topographic variables such as slope either as environmental predictors or as indirect hydrodynamic proxies [12, 13]. However, these approaches rarely integrate topographic constraints as explicit spatial filters representing effective habitat availability and inland migration potential under sea-level rise. This limitation is relevant in the Eastern Pacific, where tectonic activity and fragmented low-elevation coastal areas constrain mangrove persistence and landward migration [22, 23]. Consequently, climate-only projections may overestimate future expansion in coastal regions where suitable inland space is spatially restricted [8, 26, 27]. Because regional responses depend on the interaction between climatic conditions and topographic constraints [14, 15, 16, 28], regional assessments are necessary to identify coherent spatial trends and support conservation and adaptation strategies under climate change [18, 19, 20].

Accordingly, we used ecological niche modeling to evaluate trends in the potential distribution of three dominant mangrove species (*Avicennia germinans*, *Laguncularia racemosa*, and *Rhizophora mangle*) under six CMIP6 climate scenarios by integrating topographic constraints as a post-modeling filter representing effective habitat availability. We expected contraction trends to be concentrated in tropical ecoregions, whereas inland expansion would occur primarily in low-relief coastal systems at latitudinal margins.

Material and methods

Study area and species selection

The study area extends from southern California (USA) to northern Peru (34°28’ N – 5°57’ S), encompassing 14 ecoregions grouped into three biogeographic provinces: the Warm Temperate Northeast Pacific Province within the Temperate Northern Pacific realm and the Tropical Eastern Pacific and the Galápagos provinces within the Tropical Eastern Pacific realm [29] (Fig. 1). The climatic gradient ranges from dry and semi-arid conditions at the northern and southern extremes to humid and sub-humid tropical climates in the low-latitude zones [30] (Fig. 1). Oceanographic conditions are influenced

by the cold California and Humboldt currents at the northern and southern margins, respectively, and by the Costa Rica Current and the Equatorial Countercurrent in the tropical regions [7, 8, 31]. The coastal margin is tectonically active and characterized by fragmented low-elevation coastal areas and abrupt topographic gradients [22, 32] (Fig. S4).

We selected three of the six species distributed in the study area: *A. germinans, R. mangle*, and *L. racemosa*. These species exhibit a wide geographic distribution, structural dominance, and contrasting physiological tolerance to climatic variability [15, 25, 33], making them suitable indicators of climate change impacts on mangrove communities in the region. *R. mangle* and *L. racemosa* reach their northernmost distribution limit in the central Baja California peninsula (26°48’ N), while *A. germinans* reaches its northernmost limit farther south, at 25°47’ N. In the Gulf of California, all three species extend northward to Sonora (30°18’ N), and their southernmost limit is in Tumbes, Peru (3°26’ S). The remaining species (*A. bicolor*, *R. racemosa*, and *Pelliciera rhizophorae*) exhibit more restricted distributions confined to Central America and northern South America. *P. rhizophorae* is endemic and the sole representative of its genus [25, 33].

Presence records and accessible area (M)

Given the distributional scope of the selected species, we restricted the analysis to records from the Eastern Pacific. This decision is supported by documented genetic and physiological differences between mangrove populations from the Pacific and Atlantic basins [24, 34, 35, 36], which support treating the Eastern Pacific as a distinct biogeographic unit for ecological niche modeling.

We obtained the presence records for the three species from the Global Biodiversity Information Facility portal (www.gbif.org, accessed in 2022). Records were curated to ensure geographic and ecological consistency by removing duplicated locations and applying a spatial thinning threshold of three kilometers to reduce spatial autocorrelation and minimize model overfitting [37].

The accessible area (M) was defined following [38] as the geographic space potentially reachable by the species over ecologically relevant time periods and delimiting the environmental conditions available for model calibration. M was not restricted to the current distribution and included areas with evidence of historical accessibility based on palynological records. Mid-Holocene records document the presence of *R. mangle* and *L. racemosa* in southern California [39]. Additionally, climatically suitable areas have been identified north of Punta Eugenia [15], and successful experimental introductions have been reported in San Diego Bay (USA) [17]. These records support the inclusion of northern Pacific regions within M under a biogeographic accessibility framework.

To define M, we used *Warm Temperate Northeast Pacific, Tropical Eastern Pacific*, and *Galápagos* provinces [29], considering both filtered occurrence records and mid-Holocene palynological evidence [39]. Because mangroves have historically occupied the Warm Temperate Northeast Pacific province, southern California (USA) was established as the northern limit of M. We additionally defined a coastal

strip ≤ 50 km inland from the shoreline to include major coastal plains associated with mangrove development, such as Marismas Nacionales and insular areas in Baja California Peninsula in Mexico, as well as the Gulf of Guayaquil (Ecuador) [2, 40]. This approach ensured a continuous calibration region and avoided artificial fragmentation that could bias model outputs due to incomplete representation of environmental gradients [38]. This procedure resulted in a shared accessible area (M) for the three species, supported by their broad co-occurrence across tropical and subtropical coastal environments and overlapping environmental requirements [25, 33].

Variables selection and climate change scenarios

We developed species-specific sets of climatic variables to characterize climatic niches. Bioclimatic variables were obtained from WorldClim v2.1 portal [41] at a resolution of 30 arcseconds (~ 1 km² at the equator). Four variables (BIO8, BIO9, BIO18, BIO19) were excluded due to irregularities in the continuity of their values [42]. We then used the terra package [43] in R to extract the values of the remaining 15 variables for each species' occurrence records and to conduct a Pearson correlation test. Subsequently, we generated various sets of climatic variables with correlation coefficients < |0.8|, a threshold commonly used in ecological niche modeling [44], and selected variables considered ecologically significant for mangrove distribution [4, 45] (Fig. S1). Consequently, we produced five variable sets for *A. germinans* and *R. mangle* and three for *L. racemosa* (Table S1). The variables were restricted to the species' accessible area, using ArcGIS Pro 3.2 [46].

We evaluated three CMIP6 global circulation models (GCMs), three Shared Socio-economic Pathways (SSPs), and two temporal intervals, 2050 (2041–2060) and 2070 (2061–2080). The selected GCMs were EC-Earth Consortium (EC-Earth3-Veg), Max Planck Institute of Meteorology, Germany (MPI-ESM1-2-HR), and Meteorological Research Institute, Japan (MRI-ESM2-0), chosen for their robust climate performance and reduced temperature bias under present conditions [47]. The SSPs were SSP2–4.5, SSP3–7.0, and SSP5–8.5, representing intermediate, high, and very high emissions trajectories based on distinct socioeconomic assumptions [48, 49]. The combination of SSPs and temporal intervals produced six CMIP6 climate scenarios for each species. To reduce inter-model uncertainty, we developed a consensus model that retained only those areas where all three GCMs agreed on the potential distribution.

Model Development and Evaluation

To create the niche models, we randomly partitioned the presence records for each species, using 70% for the model training and 30% for the validation. We utilized the R package kuenm [50], which facilitates the testing and evaluation of candidate models constructed from multiple combinations of Maxent algorithm settings [51], including variable sets, feature classes, and the model flexibility (regularization multipliers). This approach enabled the assessment of 1,099 candidate models (315 for *A. germinans*, 294 for *L. racemosa*, and 490 for *R. mangle*). Candidate models were evaluated using three criteria:

statistical significance, biological performance, and model complexity. Statistical significance was assessed using a partial ROC curve from which the AUC ratio was derived (AUC ratio > 1). Biological performance was evaluated using the omission rate, which quantifies the percentage of test records not predicted by the model (OR ≤ 5%), whereas model complexity was evaluated using the difference in Akaike Information Criterion (dAIC < 2). Final models were selected based on overall performance across all three criteria.

Following model selection, we generated 10 replicated ecological niche models and projected them onto climate change scenarios without extrapolation. To derive the potential distribution model for each species, we utilized the median across the 10 replicates and transformed Maxent's logistic output into a binary presence/absence format. We used the 10th percentile of each species' training records as the threshold criterion. Consequently, results beneath the threshold were categorized as absence, and values equal to or above the threshold were categorized as presence. The procedure was executed for contemporary models and for each climate change scenario.

Topographic post-processing

To reduce commission errors associated with topographic heterogeneity in the study area (Fig. S4), we applied a topographic filter to constrain current and future (2050, 2070) projections of mangrove distribution. This filter combined low-elevation coastal zone (≤ 10 m) and gentle slope threshold (≤ 2%) and was applied to binary presence/absence models. Resulting maps were intersected with the topographic suitability layer to derive climatic and topographic distribution areas for each species.

These thresholds delineate low-lying coastal plains associated with tidal flooding, sediment accumulation, and hydrological connectivity, conditions linked to mangrove establishment and landward migration under sea-level rise [52]. The selected elevation range encompasses: (i) current mangrove distribution areas (≤ 5–6 m), (ii) adjacent coastal zones with potential for landward migration, and (iii) relict mangrove occurrences associated with ancient coastlines (≤ 10 m) [6, 25, 53].

Consequently, we conducted a geographical overlay analysis using the same resolution as the climate models (30 arc-seconds). Elevation data were obtained from WorldClim v2.1 portal [41], and the slope was computed from this data. All procedures were performed in ArcGIS Pro 3.2 [46]. Elevation and slope were incorporated during post-processing to reduce multicollinearity, given the strong association between elevation and climatic variables. The combined use of the elevation and slope improved the identification of topographically suitable areas. Both variables were assumed to remain constant across the temporal scenarios.

Analysis of distribution trends

To estimate the current and projected distribution, we generated a consensus model retaining only areas where all three global circulation models (GCMs) agreed on potential distribution and that

simultaneously satisfied topographic suitability (Climate ∩ Topography).

Distribution change was then assessed by reclassifying future climate rasters as values of 0 (absent) and 10 (present), while contemporary rasters were coded as 0 (absent) and 1 (present). Raster sums between contemporary models and each future climate scenario identified areas of loss (1), gain (10), and stability (11). Distribution areas were quantified by pixel counts. Similarly, we assessed the extent of the current species co-distribution. All procedures were executed in R version 3.6.6 [54] and ArcGIS Pro 3.2 [46].

Distribution trends were analyzed at regional, provincial, and ecoregional scales across the Eastern Pacific. Ecoregional analyses were used to identify representative spatial patterns within provinces rather than as independent analytical units. Therefore, we conducted an integrated evaluation of distribution change trends considering three indicators: i) type (stability, loss, and gain), ii) magnitude (pixel area), and iii) consistency, defined as persistence across climate trajectories. Dominant change patterns at the ecoregional level were assigned according to the relative contribution and spatial predominance of stability, loss, and gain categories. Categories such as “stability-dominated”, “stability-gain”, and “loss-dominated” were interpreted qualitatively based on the prevailing trend and the relative magnitude of secondary change components. Consistency was classified as early when trends originated under intermediate trajectories (SSP3–7.0), late when they appeared only under high-emission trajectories (SSP5–8.5), and persistent when maintained across all three trajectories, indicating robustness along the climate hazard gradient.

Results

Models evaluation and topographic correction

A total of 1,248 records were obtained, including 379 for *A. germinans*, 429 for *L. racemosa*, and 440 for *R. mangle*. These records covered the current distributional range of the three species across the Eastern Pacific. Among the potential models assessed for each species, only one satisfied the kuenm evaluation criteria, demonstrating low omission rates (OR ≤ 5%) and statistical significance (AUC ratio > 1) (Table S2). The climatic variables that most strongly influenced the models for the three species included mean annual temperature, mean diurnal temperature range, minimum temperature of the coldest month, precipitation of the wettest month, and precipitation of the driest month (Table S3). The topographic correction substantially reduced the projected potential distribution of the three species, retaining an average of 18.9% of the climate-only projected area under current conditions (Table S4, Fig. 2). A comparable trend was observed in the climate change scenarios, with an average remaining area of 16.1% projected for 2050 and 17.1% for 2070, each representing the total area estimated for their respective periods (Table S4).

Regional distribution trends

The regional distribution models under current conditions exhibited similar spatial patterns for the three species, with latitudinal range limits spanning from Southern California (USA) to Punta Aguja (PER) (34°21’ N – 5°58’ S), covering most of the accessible area. Similarly, the models showed a high degree of regional overlap among species (86.9%) indicating substantial co-distribution. *L. racemosa* exhibited slightly broader latitudinal range limits (48,547 pixels) compared to *A. germinans* (46,502 pixels) and *R. mangle* (45,850 pixels). Climate scenario models indicate nearly identical latitudinal ranges for all three species, with a decrease of 9.8% to 35.3% relative to the current potential distribution (Table S5).

Future climate scenarios maintained nearly identical latitudinal ranges for all three species, while projected changes were primarily expressed as internal spatial reconfiguration within the current range. Stability was the dominant trend (48.8% to 66.8%), followed by loss (21.1% to 39.7%), both primarily concentrated in tropical portions of the range. In contrast, gain trends were less frequent (6.9% to 16.9%) and were mainly located at latitudinal extremes and along the landward margin, associated with the emergence of new inland areas (Fig. 3; Table S6). These results indicate that regional trends are not driven by latitudinal shifts but by internal spatial changes within the current distribution range, where contraction in some areas coexists with gains into new zones (Fig. S5-S22).

At the species level, average change trends showed similar spatial patterns but differed in magnitude. *R. mangle* exhibited the lowest stability (53.6%), the highest loss (30.7%), and the highest gain (15.7%), indicating species-specific sensitivity to climate change (Table S6). *A. germinans* showed moderate stability (60.2%), the lowest loss (27.9%), and intermediate gain (12.1%). In contrast, *L. racemosa* showed a slightly higher stability (60.5%), intermediate loss (29.4%), and the lowest gain trends (10.1%) (Table S6).

Provincial and ecoregional trends

At the provincial level, the current potential distribution of the three species showed strongly asymmetric patterns (Fig. 4), with a greater average extent in the Tropical Eastern Pacific (57%), followed by the Warm Temperate Northeast Pacific (42.3%), while the Galápagos represented a marginal proportion (0.7%) of the total area (Table 1; Fig. S5-S22).

Under future scenarios, contrasting spatial and temporal responses emerged among provinces. The Galápagos exhibited complete stability across all scenarios (100%), with no projected gains or losses, indicating a persistent stability signal (Fig. 4; Table S7). Similarly, the WTNP, located at the northern limit of the distribution, showed a strong dominance of stable areas (74.9%), accompanied by a notable gain component (21.7%) and minimal losses (3.4%) (Table S7). Importantly, losses in this province were scenario-dependent and temporally delayed, emerging only under high-emission scenarios and predominantly toward 2070, indicating a late-emerging response and high persistence under moderate climate trajectories. In contrast, the Tropical Eastern Pacific displayed a persistent trend of distribution loss, with an average reduction of 53% in distribution area, consistent with loss-dominated trends across ecoregions (Table 1; Table S7). These losses were consistently detected across all scenarios, including

moderate trajectories, indicating an early-emerging and persistent signal of contraction. Stability remained moderate (42.4%), while gains were limited (4.6%) (Fig. 4, Table S7).

At the ecoregional scale, these contrasts became more pronounced and spatially structured (Table 1, Table S8). Within the WTNP, the Cortezian ecoregion emerged as a stability–gain system and a core of potential expansion and persistence, concentrating the largest areas of both stability and gain under the moderate scenario and across scenario averages (Table 1; Table S9; Fig. S5-S10). The Magdalena Transition and Southern California Bight ecoregions also exhibited predominantly stability-dominated systems with moderate gains (Table 1), reinforcing the role of this province as a regional stability refugium with delayed response dynamics (Table 1; Table S9; Fig. S5-S10). On the other hand, within the TEP, losses were widespread along the coastal margin (Table 1; Table S8; Fig. S11–S21), with the highest magnitudes observed in the Chiapas–Nicaragua and Panama Bight ecoregions, which functioned as loss-dominated contraction hotspots with early and persistent signals. The Mexican Tropical Pacific and Nicoya ecoregions also exhibited substantial losses and null gain trends (Table 1). In contrast, the Guayaquil ecoregion showed a strong stability-gain trend, representing a system with inland expansion potential within an otherwise contracting province.

Oceanic ecoregions such as Revillagigedo remained stable, while Clipperton and the Cocos Islands showed no potential distribution under current and future conditions (Table 1). Similarly, the Galápagos Islands province remained stable across its three ecoregions, with no projected gains or losses.

Discussion

Regional trends and spatial configuration

Our results indicate that the potential distribution of *A. germinans, L. racemosa, and R. mangle* across the Eastern Pacific maintained relatively stable latitudinal boundaries and high spatial overlap under future climate scenarios. Thus, projected changes are primarily expressed as internal spatial reconfiguration within the current range rather than through poleward expansion. At the regional scale, the Warm Temperate Northeast Pacific functions as a zone of relative stability and inland expansion, whereas the Tropical Eastern Pacific concentrates persistent contraction trends. These patterns partially align with global projections [12, 13] but reveal region-specific responses mediated by the interaction between climatic conditions and topographic constraints on effective habitat availability. Despite the presence of climatically and topographically suitable conditions beyond current northern limits, no clear poleward expansion was projected, suggesting that propagule dispersal constraints may limit range expansion in the Eastern Pacific [17, 21].

Inland expansion was strongly constrained by the discontinuous distribution of low-elevation coastal plains along this tectonically active margin [22]; Fig. S4). Consequently, climate-only projections not necessarily represent effective habitat availability because landward migration depends on sufficient low-relief coastal space [55]. This limitation is consistent with the fragmented contemporary mangrove

distribution across the Eastern Pacific and supports the role of topographic constraints in shaping both current and projected spatial patterns [56, 57]. The topographic filter retained only 18.9% of the areas projected under climate-only conditions, indicating that most climatically projected areas lack the topographic conditions required for effective mangrove persistence and inland migration.

At the latitudinal extremes, changes in precipitation and increases in minimum winter temperature reduce thermal constraints on mangrove establishment [7, 8, 14]. Additionally, sea-level rise and El Niño events may amplify these processes by temporarily increasing coastal humidity and inundation, facilitating the formation of supratidal habitats suitable for inland colonization, particularly in low coastal plains of arid zones [58].

In contrast, the contraction observed in the Tropical Eastern Pacific reflects higher environmental sensitivity, where temperature becomes less limiting and other stressors become more relevant. In these regions, increased climatic variability and reduced or irregular precipitation and limited availability of low-elevation inland space interact to constrain mangrove persistence and reduce their capacity for expansion [7, 8, 14]. These findings highlight the importance of topographic constraints in mediating regional mangrove responses to climate change [23, 59].

Provincial and ecoregional responses

The Eastern Pacific exhibited a strongly asymmetric regional response structured by contrasting trends of stability, loss, and gain across provinces and ecoregions (Table 1). Tropical sectors showed persistent contraction trends, whereas peripheral and arid regions exhibited greater stability and inland expansion potential. These asymmetric responses were associated with regional differences in climatic variability and the availability of low-relief coastal systems capable of supporting inland migration. In tropical regions, higher temperature and precipitation variability increase environmental stress and may push mangrove systems closer to ecological thresholds [8, 60]. Combined with fragmented coastal plains, these conditions may reduce mangrove persistence and limit inland migration. In contrast, peripheral regions with extensive low-relief coastal plains exhibited lower climate exposure and greater stability, favoring inland expansion potential (Fig. S4) [7, 8].

These results suggest that regional responses are not driven solely by climatic conditions, but also by the spatial availability of low-elevation coastal systems capable of supporting landward migration under sea-level rise. Under these conditions, limited inland accommodation space may promote spatial responses consistent with coastal squeeze, particularly along tectonically active coastal margins [27]. This limitation may be further exacerbated by anthropogenic barriers that restrict landward migration, thereby reducing mangrove persistence [8].

The Tropical Eastern Pacific, which contains the largest extent and higher genetic diversity [61, 62], exhibited the highest projected losses (~ 53%) and persistent contraction trends across scenarios. Most ecoregions functioned as loss-dominated systems with negligible or null gains, particularly Chiapas–Nicaragua, the Mexican Tropical Pacific, and Nicoya (Table 1), while the Guayaquil ecoregion exhibited a

stability–gain pattern, associated with the presence of extensive low-relief coastal plains. These spatial differences reinforce the importance of low-relief coastal plains in mediating regional responses to climate change.

In contrast, the Warm Temperate Northeast Pacific showed high stability and substantial gains, indicating greater potential for persistence and inland expansion. Ecoregions such as the Cortezian functioned as expansion-prone areas associated with extensive low-relief coastal plains. However, future inland migration in these regions may still be limited by anthropogenic pressures such as coastal infrastructure and land-use change [8].

Oceanic ecoregions such as Clipperton and the Cocos Islands show no potential distribution under current or future conditions (Table 1), while Revillagigedo represents a marginal system with minimal change. Similarly, the Galápagos Province exhibits complete stability but no potential expansion (Table S7), reflecting a system with high persistence but limited accommodation space, which may constrain its adaptive capacity under future environmental change.

Species responses and ecological differentiation

Although the three species analyzed exhibit broadly similar regional spatial patterns, differences in stability, loss, and gain reflect species-specific sensitivities to environmental change. These differences indicate that mangrove responses are not only spatially structured but also taxonomically differentiated, with potential implications for community composition and ecosystem functioning.

R. mangle exhibited the lowest stability and the highest loss, indicating greater sensitivity to projected environmental changes. Although gains were identified, these are likely constrained by its strong dependence on intertidal conditions and hydrological connectivity [63], which may limit its capacity to effectively occupy newly suitable inland areas. In contrast, *A. germinans* showed the highest stability and moderate gains, suggesting greater resilience under changing conditions. Its broader tolerance to salinity and hydrological variability may facilitate inland expansion, as observed in empirical studies [58, 64]. *L. racemosa* displayed an intermediate pattern in terms of stability, loss, and gain, indicating moderate sensitivity to climate change [64].

Future mangrove dynamics in the Eastern Pacific may therefore involve not only spatial changes in potential distribution, but also shifts in species dominance and community structure, with potential consequences for ecosystem functioning and adaptive capacity under climate change [28, 65, 66].

Limitations and uncertainty

Projected distributions should be interpreted as spatially constrained potential distributions rather than realized future occupancy. Although the integration of topographic constraints reduces overestimation associated with climate-only projections, future mangrove establishment and persistence remain dependent on additional ecological and geomorphological processes not explicitly incorporated into the models, including dispersal dynamics, sedimentation, hydrological connectivity, and soil conditions [6,

63, 64]. In addition, the topographic filter assumes static elevation conditions and does not incorporate future geomorphological dynamics such as sediment accretion, erosion, or local shoreline change that may modify effective habitat availability through time [6, 59, 63]. Finally, anthropogenic pressures such as coastal infrastructure and land-use change may further restrict inland migration and reduce the effective availability of accommodation space, particularly in densely modified coastal systems [8, 27, 67].

Conservation implications under climate change

The identification of loss hotspots, climate refugia, and areas with inland expansion potential provides a spatially explicit framework for conservation planning under climate change. The results indicate that the Tropical Eastern Pacific, particularly the Chiapas–Nicaragua and Panama Bight ecoregions, will face the greatest losses and reduced adaptive capacity. These areas should be prioritized for conservation and restoration strategies aimed at enhancing resilience, maintaining connectivity, and reducing additional anthropogenic pressures. Given that this region harbors the highest mangrove extent and genetic diversity [61, 62], its vulnerability represents a significant ecological and evolutionary concern. This spatial framework aligns with the Kunming-Montreal Global Biodiversity Framework by supporting the identification of priority areas for restoration and conservation while highlighting that topographic constraint may limit the feasibility of achieving these targets under climate change.

In contrast, the Warm Temperate Northeast Pacific (WTNP) and the Galápagos Province exhibited relative stability, although with distinct ecological implications. In the WTNP, mangroves showed high stability and inland expansion potential, suggesting that low-elevation coastal plains may support future inland migration under climate change. However, this potential depends on the protection of low-elevation coastal areas that may facilitate inland migration. Conservation strategies in these areas should prioritize the preservation of low-elevation coastal plains and prevent land-use changes that may restrict landward migration [27]. Within this context, areas such as the Southern California Bight represent systems where suitable environmental conditions exist and historical evidence supports mangrove presence [39]. In these cases, these systems require ecological and socio-environmental evaluation [17]. In contrast, the Galápagos Province represents a highly stable system with no projected expansion, reflecting strong persistence but potential for spatial expansion. Despite current stability, these systems may be vulnerable to future environmental change due to limited capacity for expansion.

Overall, the results highlight that the availability of accommodation space is a key factor regulating mangrove persistence and expansion. Where topographic constraints limit inland migration, even under projected increases in potential distribution, mangrove systems may experience conditions consistent with coastal squeeze, particularly when compounded by anthropogenic pressures such as coastal infrastructure and land-use change [8, 27].

From a management perspective, these findings highlight the need to incorporate dynamic habitat processes into coastal planning frameworks, including the protection of inland migration corridors and adaptive coastal zoning strategies under sea-level rise [8, 60]. Failing to account for these processes

may exacerbate habitat loss by limiting the capacity of mangrove ecosystems to adjust to changing environmental conditions.

Conclusions

Under climate change scenarios, the potential distribution of *A. germinans*, *L. racemosa*, and *R. mangle* in the Eastern Pacific is projected to retain stable latitudinal limits and substantial interspecific overlap, while undergoing pronounced internal spatial reconfiguration within the current range. Topographic filtering retained only a small fraction of the climate-only projected areas, highlighting the strong spatial limitations imposed by the fragmented distribution of low-elevation coastal systems in the Eastern Pacific. Contraction trends in tropical regions and potential inland expansion at latitudinal margins indicate that future mangrove dynamics will be governed primarily by internal spatial reconfiguration rather than by poleward shifts. At broader scales, this restructuring is asymmetric: the Warm Temperate Northeast Pacific emerges as a zone of relative stability and expansion, whereas the Tropical Eastern Pacific concentrates the highest levels of contractions. These patterns reflect the interaction between climatic conditions and topographic constraints, emphasizing the central role of accommodation space in mediating realized distributional change.

This asymmetry is further expressed at the ecoregional scale, where contraction hotspots dominate tropical systems such as the Mexican Tropical Pacific and Chiapas–Nicaragua, while regions such as the Guayaquil Gulf and the Warm Temperate Northeast Pacific exhibit stability–gain patterns associated with the availability of low-relief coastal plains. In contrast, the Galápagos Province remains highly stable but shows negligible expansion potential, reflecting limited capacity for spatial adjustment. Superimposed on these spatial patterns are species-specific responses: *R. mangle* appears most vulnerable, *A. germinans* most resilient, and *L. racemosa* intermediate, suggesting potential shifts in community structure and ecosystem functioning.

Collectively, these results indicate that mangrove persistence in the Eastern Pacific will depend not only on climatic conditions but also on the availability of effective habitat shaped by topographic constraints and anthropogenic pressures. Conservation strategies should therefore move beyond static range projections and explicitly incorporate the protection of inland accommodation space and the facilitation of landward migration under climate change.

Declarations

Author contributions

P.G.Z. conceived the study, performed the investigation and formal analysis, developed the methodology, and wrote the original draft and subsequent revisions of the manuscript. F.A.T.C. developed the methodology, performed formal analysis, implemented the software, performed visualizations, and wrote and revised the manuscript. J.R.R. developed the methodology, validated the data, performed

visualizations, and edited the manuscript. S.E.L.C. wrote and revised the manuscript. D.A.P.G. wrote and revised the manuscript.

All authors reviewed and approved the final manuscript

Additional information

Competing interests

The authors declare no competing interests.

Funding

This work was supported through a collaboration agreement between the Consejo Sudcaliforniano de Ciencia y Tecnología, Mexico (COSCYT) and the Centro de Investigaciones Biológicas del Noroeste, Mexico (CIBNOR) under agreement CAR/22/2024.

Data availability

Curated occurrence records and topographic constraint layers generated and analyzed during this study are available through a private Figshare review link: https://figshare.com/s/13f036a284db51d533a2. Upon acceptance, the repository will be made publicly available and assigned a permanent DOI.Original occurrence records were obtained from the Global Biodiversity Information Facility (GBIF), and climate datasets were obtained from WorldClim v2.1. Additional environmental and topographic datasets were derived from publicly available sources cited in the manuscript. Derived distribution trend layers and additional spatial analytical outputs generated during the current study are available from the corresponding author upon reasonable request.

References

1. Lovelock, C. E. et al. Mangrove biodiversity and ecosystem services. *Nat. Rev. Biodivers.* **1**, 772–787. https://doi.org/10.1038/s44358-025-00103-3 (2025).
2. Bunting, P. et al. Global mangrove extent change 1996–2020: Global Mangrove Watch version 3.0. *Remote Sens.* **14**, 3657. https://doi.org/10.3390/rs14153657 (2022).
3. Worthington, T. & Spalding, M. Mangrove Restoration Potential: A global map highlighting a critical opportunity. Apollo - University of Cambridge Repository. (2019). https://doi.org/10.17863/CAM.39153
4. Saintilan, N. et al. Thresholds of mangrove survival under rapid sea level rise. *Science* **368**, 1118–1121. https://doi.org/10.1126/science.aba2656 (2020).
5. IPCC. *Climate Change 2021: The Physical Science Basis*. Contribution of Working Group I to the Sixth Assessment Report of the Intergovernmental Panel on Climate Change. (2021). https://doi.org/10.1017/9781009157896

6. Xie, D., Kleinhans, M. G., Zhou, Z., Leuven, J. R. F. W. & Stive, M. J. F. Implications of coastal conditions and sea-level rise on mangrove vulnerability: A bio-morphodynamic modelling study. *J. Geophys. Res. Earth Surf.* **127**, e2021JF006301. https://doi.org/10.1029/2021JF006301 (2022).
7. Alongi, D. M. The impact of climate change on mangrove forests. *Curr. Clim. Change Rep.* **1**, 30–39. https://doi.org/10.1007/s40641-015-0002-x (2015).
8. Ward, R. D., Friess, D. A., Day, R. H. & Mackenzie, R. A. Impacts of climate change on mangrove ecosystems: a region by region overview. *Ecosyst. Health Sustain.* **2**, e01211. https://doi.org/10.1002/ehs2.1211 (2016).
9. Alongi, D. M. Mangrove forests: resilience, protection from tsunamis, and responses to global climate change. *Estuar. Coast Shelf Sci.* **76**, 1–13. https://doi.org/10.1016/j.ecss.2007.08.024 (2008).
10. Barbier, E. B. et al. The value of estuarine and coastal ecosystem services. *Ecol. Monogr.* **81**, 169–193. https://doi.org/10.1890/10-1510.1 (2011).
11. Neumann, B., Vafeidis, A. T., Zimmermann, J. & Nicholls, R. J. Future coastal population growth and exposure to sea-level rise and coastal flooding—a global assessment. *PLoS One*. **10**, e0118571. https://doi.org/10.1371/journal.pone.0118571 (2015).
12. Record, S., Charney, N. D., Zakaria, R. M. & Ellison, A. M. Projecting global mangrove species and community distributions under climate change. *Ecosphere* **4**, 1–23. https://doi.org/10.1890/ES12-00296.1 (2013).
13. Gouvêa, L. P. et al. Global impacts of projected climate changes on the extent and aboveground biomass of mangrove forests. *Divers. Distrib.* **28**, 2349–2360. https://doi.org/10.1111/ddi.13631 (2022).
14. Cavanaugh, K. C. et al. Climate-driven regime shifts in a mangrove-salt marsh ecotone over the past 250 years. *Proc. Natl Acad. Sci. USA* 116, 21602–21608 (2019). https://doi.org/10.1073/pnas.1902181116
15. Bardou, R., Parker, J. D., Feller, I. C. & Cavanaugh, K. C. Variability in the fundamental versus realized niches of North American mangroves. *J. Biogeogr.* **48**, 160–175. https://doi.org/10.1111/jbi.13990 (2021).
16. Bardou, R. et al. Projected changes in mangrove distribution and vegetation structure under climate change in the southeastern United States. *J. Biogeogr.* **51**, 2285–2297. https://doi.org/10.1111/jbi.14985 (2024).
17. Cavanaugh, K. C., Carrol, D., Bardou, R. & Van der Stocken, T. Dispersal limits poleward expansion of mangroves on the west coast of North America. *Ecography* **2024**, e07288. https://doi.org/10.1111/ecog.07288 (2024).
18. Pechi, M. et al. Species distribution modelling to support forest management: A literature review. *Ecol. Model.* **411**, 108817. https://doi.org/10.1016/j.ecolmodel.2019.108817 (2019).
19. Thurman, L. L. et al. Application of adaptive capacity assessments to inform natural resource management under climate change. *Conserv. Biol.* **36**, e13838. https://doi.org/10.1111/cobi.13838

(2022).
20. Xu, X. et al. Global distribution and decline of mangrove coastal protection extends far beyond area loss. *Nat. Commun.* **15**, 10267. https://doi.org/10.1038/s41467-024-54349-0 (2024).
21. Van der Stocken, T. et al. A general framework for propagule dispersal in mangroves. *Biol. Rev.* **94**, 1547–1575. https://doi.org/10.1111/brv.12514 (2019).
22. Inman, D. L. & Nordstrom, C. E. On the tectonic and morphologic classification of coasts. *J. Geol.* **79**, 1–21. https://doi.org/10.1086/627583 (1971).
23. Woodroffe, C. D. Mangrove sediments and geomorphology. In *Tropical Mangrove Ecosystems* (eds Robertson, A. I. & Alongi, D. M.) 7–41 (American Geophysical Union, 1992). https://doi.org/10.1029/CE041p0007
24. Nettel, A. & Dodd, R. S. Drifting propagules and receding swamps: genetic footprints of mangrove recolonization and dispersal along tropical coasts. *Evolution* **61**, 958–971. https://doi.org/10.1111/j.1558-5646.2007.00070.x (2007).
25. Tomlinson, P. B. *The Botany of Mangroves*Cambridge University Press, (2016). https://doi.org/10.1017/CBO9781139946575
26. Gilman, E., Ellison, J., Duke, N. C. & Field, C. Threats to mangroves from climate change and adaptation options: A review. *Aquat. Bot.* **89**, 237–250. https://doi.org/10.1016/j.aquabot.2007.12.009 (2008).
27. Schuerch, M. et al. Future response of global coastal wetlands to sea-level rise. *Nature* **561**, 231–234. https://doi.org/10.1038/s41586-018-0476-5 (2018).
28. Saintilan, N., Wilson, N. C., Rogers, K., Rajkaran, A. & Krauss, K. W. Mangrove expansion and salt marsh decline at mangrove poleward limits. *Glob Change Biol.* **20**, 147–157. https://doi.org/10.1111/gcb.12341 (2014).
29. Spalding, M. D. et al. Marine ecoregions of the world: a bioregionalization of coastal and shelf areas. *Bioscience* **57**, 573–583. https://doi.org/10.1641/B570707 (2007).
30. Beck, H. E. et al. Present and future Köppen-Geiger climate classification maps at 1-km resolution. *Sci. Data*. **5**, 180214. https://doi.org/10.1038/sdata.2018.214 (2018).
31. Kessler, W. S. The circulation of the eastern tropical Pacific: a review. *Prog Oceanogr.* **69**, 181–217. https://doi.org/10.1016/j.pocean.2006.03.009 (2006).
32. Velázquez-Pérez, C. et al. Geoforms and biogeography defining mangrove primary productivity: A meta-analysis for the American Pacific. *Forests* **15**, 1215. https://doi.org/10.3390/f15071215 (2024).
33. Spalding, M., Kainuma, M. & Collins, L. *World Atlas of Mangroves* (Earthscan, 2010).
34. Núñez-Farfán, J. et al. Genetic divergence among Mexican populations of red mangrove (*Rhizophora mangle*): Geographic and historic effects. *Evol. Ecol. Res.* **4**, 1049–1064 (2002).
35. Cerón-Souza, I. et al. Contrasting demographic history and gene flow patterns of two mangrove species on either side of the Central American Isthmus. *Ecol. Evol.* **5**, 3486–3499.

https://doi.org/10.1002/ece3.1569 (2015).

36. Dodd, R. S. & Afzal-Rafii, Z. Evolutionary genetics of mangroves: continental drift to recent climate change. *Trees* **16**, 80–86. https://doi.org/10.1007/s00468-001-0142-6 (2002).
37. Cobos, M. E., Jiménez, L., Nuñez-Penichet, C., Romero-Alvarez, D. & Simoes, M. Sample data and training modules for cleaning biodiversity information. *Biodivers. Inf.* **13**, 49–50. https://doi.org/10.17161/bi.v13i0.7600 (2018).
38. Barve, N. et al. The crucial role of the accessible area in ecological niche modeling and species distribution modeling. *Ecol. Model.* **222**, 1810–1819. https://doi.org/10.1016/j.ecolmodel.2011.02.011 (2011).
39. Scott, D. B., Mudie, P. J. & Bradshaw, J. S. Coastal evolution of Southern California as interpreted from benthic foraminifera, ostracodes, and pollen. *J. Foraminifer. Res.* **41**, 285–307. https://doi.org/10.2113/gsjfr.41.3.285 (2011).
40. Runfola, D. et al. geoBoundaries: a global database of political administrative boundaries. *PLoS One*. **15**, e0231866. https://doi.org/10.1371/journal.pone.0231866 (2020).
41. Fick, S. E., Hijmans, R. J. & WorldClim 2: New 1-km spatial resolution climate surfaces for global land areas. *Int. J. Climatol.* 37, 4302–4315 (2017). https://doi.org/10.1002/joc.5086
42. Booth, T. H. Checking bioclimatic variables that combine temperature and precipitation data before their use in species distribution models. *Austral Ecol.* **47**, 1506–1514. https://doi.org/10.1111/aec.13234 (2022).
43. Hijmans, R. J. terra: spatial data analysis. R package version 1.8–62. CRAN: Package terra - Spatial Data Analysis (2025).
44. Díaz-Vallejo, M. et al. Analyses of the variable selection using correlation methods: an approach to the importance of statistical inferences in the modelling process. *Ecol. Model.* **498**, 110893. https://doi.org/10.1016/j.ecolmodel.2024.110893 (2024).
45. Friess, D. A., Adame, M. F., Adams, J. B. & Lovelock, C. E. Mangrove forests under climate change in a 2°C world. Wiley Interdiscip. *Rev. Clim. Change*. **13**, e792. https://doi.org/10.1002/wcc.792 (2022).
46. ESRI. ArcGIS Pro version 3.2. (2023). https://www.esri.com/es-es/arcgis/products/arcgis-pro/overview
47. Mahony, C. R., Wang, T., Hamann, A. & Cannon, A. J. A global climate model ensemble for downscaled monthly climate normals over North America. *Int. J. Climatol*. **42**, 5871–5891. https://doi.org/10.1002/joc.7566 (2022).
48. Eyring, V. et al. Overview of the coupled model intercomparison project phase 6 (CMIP6) experimental design and organization. *Geosci. Model. Dev.* **9**, 1937–1958. https://doi.org/10.5194/gmd-9-1937-2016 (2016).
49. IPCC. Climate Change : Synthesis Report. Contribution of Working Groups I, II and III to the Sixth Assessment Report of the Intergovernmental Panel on Climate Change (IPCC, Geneva, Switzerland, 2023). (2023). https://doi.org/10.59327/IPCC/AR6-9789291691647

50. Cobos, M. E., Peterson, A. T., Barve, N. & Osorio-Olvera, L. kuenm: an R package for detailed development of ecological niche models using Maxent. *PeerJ* **7**, e6281. https://doi.org/10.7717/peerj.6281 (2019).
51. Phillips, S. J., Anderson, R. P. & Schapire, R. E. Maximum entropy modeling of species geographic distributions. *Ecol. Model.* **190**, 231–259. https://doi.org/10.1016/j.ecolmodel.2005.03.026 (2006).
52. Ellison, J. C. Vulnerability of mangroves to climate change. In Coastal Wetlands: An Integrated Ecosystem Approach (eds Perillo, G. M. E., Wolanski, E., Cahoon, D. R. & Brinson, M. M.) 491–536 (Elsevier, 2015). https://doi.org/10.1016/B978-0-444-63893-9.00015-2
53. Aburto-Oropeza, O. et al. Relict inland mangrove ecosystem reveals last interglacial sea levels. *Proc. Natl Acad. Sci*. *USA* 118 (41), e2024518118 (2021). https://doi.org/10.1073/pnas.2024518118
54. R Core Team. R: A Language and Environment for Statistical Computing. R Foundation for Statistical Computing, Vienna, Austria, (2018). https://www.R-project.org/
55. Temmerman, S. et al. Ecosystem-based coastal defence in the face of global change. *Nature* **504**, 79–83. https://doi.org/10.1038/nature12859 (2013).
56. Montes-Chaura, C. et al. IUCN Red List of Ecosystems, mangroves of the Tropical East Pacific. (2024). https://ecoevorxiv.org/repository/view/7259
57. Valderrama-Landeros, L. et al. IUCN Red List of Ecosystems, mangroves of the Warm Temperate Northeast Pacific. (2024). https://doi.org/10.32942/x2b03v
58. López-Medellín, X. et al. Oceanographic anomalies and sea-level rise drive mangroves inland in the Pacific coast of Mexico. *J. Veg. Sci.* **22**, 143–151. https://doi.org/10.1111/j.1654-1103.2010.01232.x (2011).
59. Kirwan, M. L. & Megonigal, J. P. Tidal wetland stability in the face of human impacts and sea-level rise. *Nature* **504**, 53–60. https://doi.org/10.1038/nature12856 (2013).
60. Friess, D. A. et al. The state of the world's mangrove forests: past, present, and future. *Annu. Rev. Environ. Resour.* **44**, 89–115. https://doi.org/10.1146/annurev-environ-101718-033302 (2019).
61. Sandoval-Castro, E., Muñiz-Salazar, R., Enríquez-Paredes, L. M. & Dodd, R. S. Genetic structure of red mangrove (Rhizophora mangle) along the Mexican Pacific: latitudinal variation and conservation implications. *Aquat. Bot.* **99**, 34–41. https://doi.org/10.1016/j.aquabot.2012.02.005 (2012).
62. Ochoa-Zavala, M. et al. Reduction of genetic variation when far from the niche centroid: prediction from mangrove species. *Front. Conserv. Sci.* **2**, 795365. https://doi.org/10.3389/fcosc.2021.795365 (2022).
63. Lovelock, C. E. et al. The vulnerability of Indo-Pacific mangrove forests to sea-level rise. *Proc. Natl Acad. Sci. USA* 112, 801–806 (2015). https://doi.org/10.1073/pnas.1416252112
64. Krauss, K. W. et al. Environmental drivers in mangrove establishment and early development: a review. *Glob Change Biol.* **14**, 1–15. https://doi.org/10.1111/j.1365-2486.2008.01686.x (2008).
65. Banerjee, A. K. et al. Setting the priorities straight – species distribution models assist to prioritize conservation targets for the mangroves. *Sci. Total Environ.* **806**, 150937.

https://doi.org/10.1016/j.scitotenv.2021.150937 (2022).

66. Samal, P. et al. Ensemble modeling approach to predict the past and future climate suitability for two mangrove species along the coastal wetlands of peninsular India. *Ecol. Inf.* **72**, 101819. https://doi.org/10.1016/j.ecoinf.2022.101819 (2022).
67. Goldberg, L., Lagomasino, D., Thomas, N. & Fatoyinbo, T. Global declines in human-driven mangrove loss. *Glob Change Biol.* **26**, 5844–5855. https://doi.org/10.1111/gcb.15275 (2020).

Tables

Table 1 is available in the Supplementary Files section.

Figures

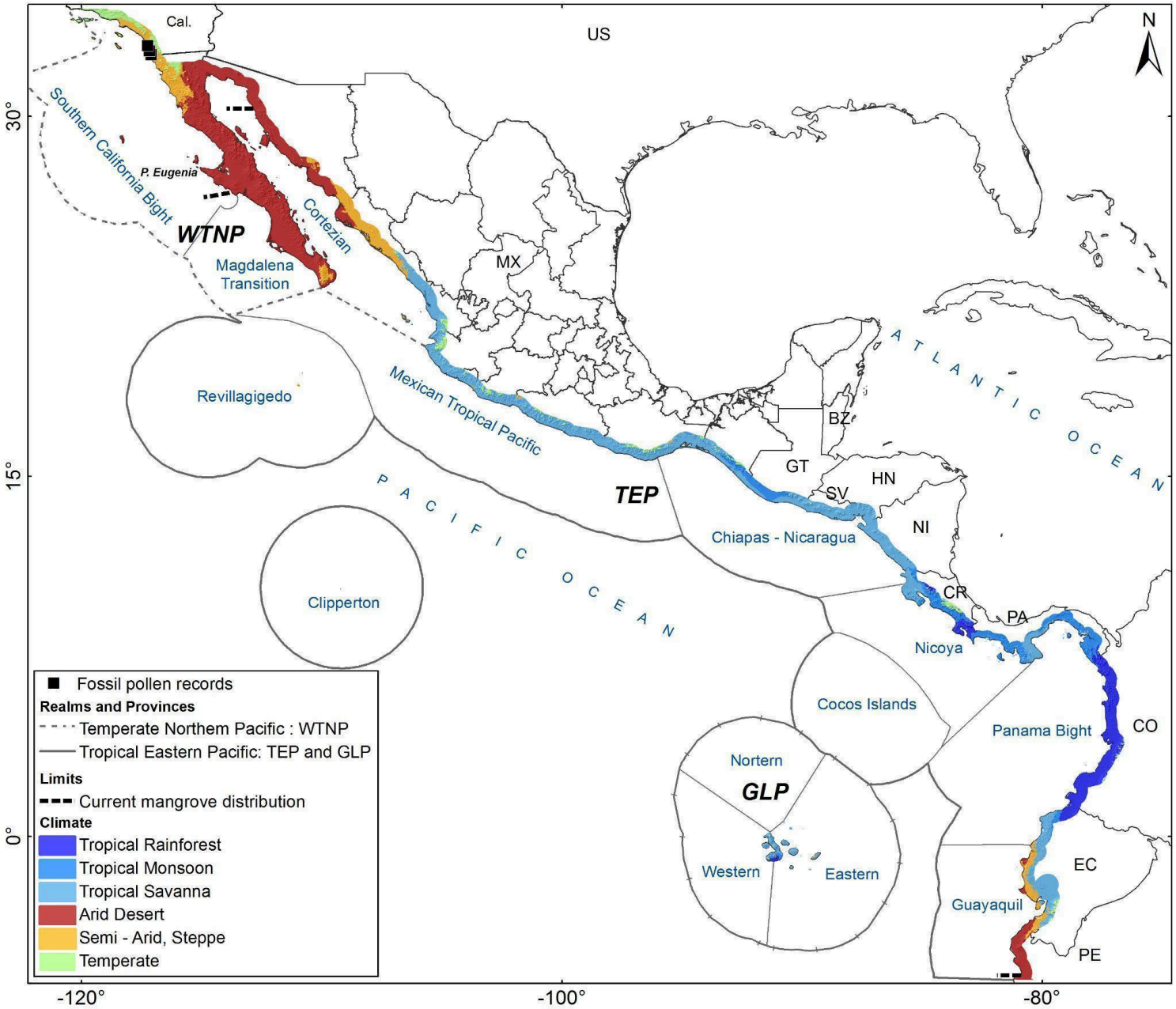

Figure 1

Calibration area used for the potential distribution models of *A. germinans, L. racemosa, and R. mangle*, across the Eastern Pacific biogeographic provinces: Warm Temperate Northeast Pacific (WTNP), Tropical Eastern Pacific (TEP), and Galápagos (GLP). Biogeographic realms and ecoregions, follow Spalding et al. [29], whereas climate types follow Beck et al. [30].

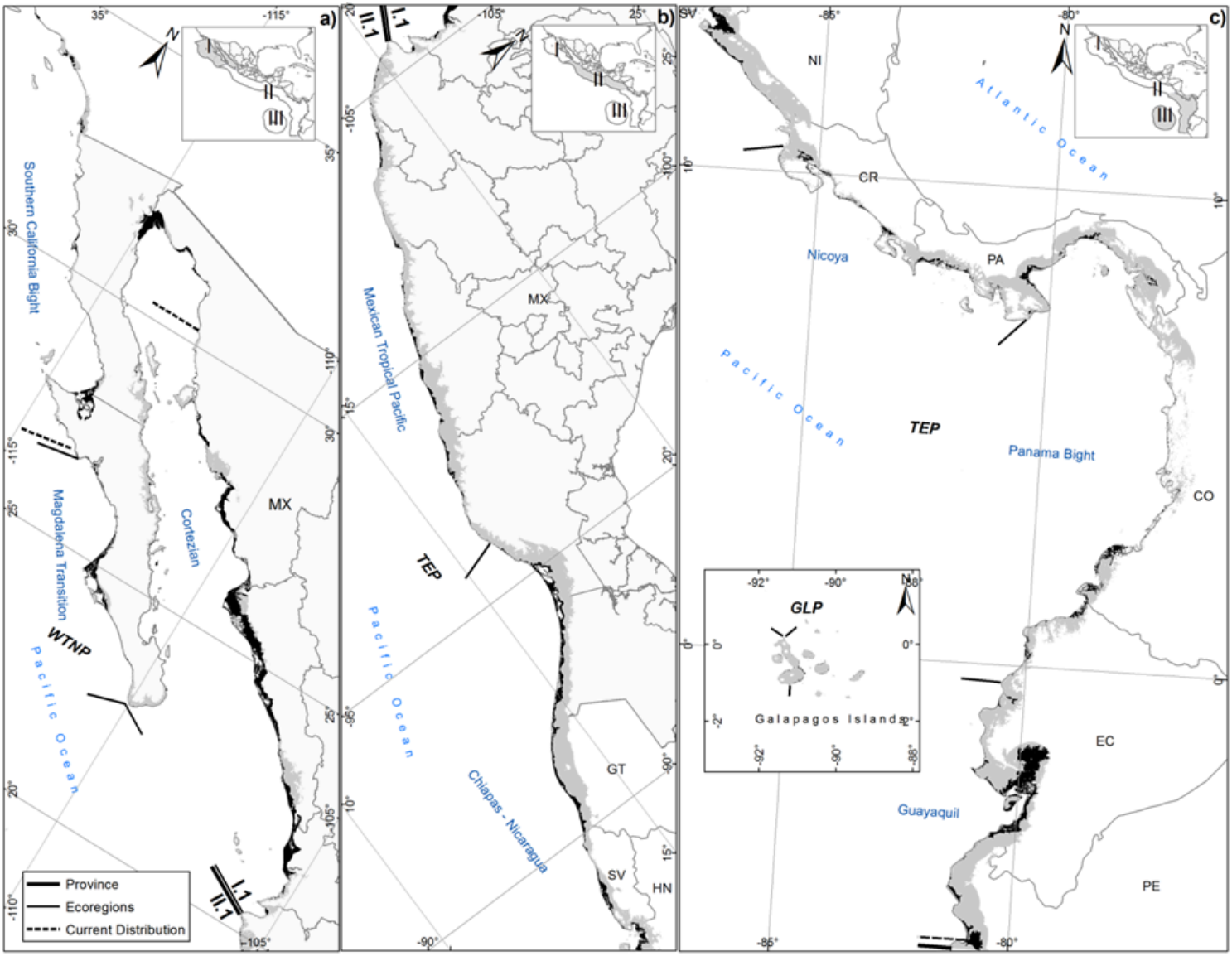

Figure 2

Current potential distribution of *L. racemosa* in the Eastern Pacific. Grey and black areas represent the climatic model prediction (258,352 pixels), whereas black areas indicate the effective habitat retained after applying the topographic filter (48,547 pixels; 18.8%).

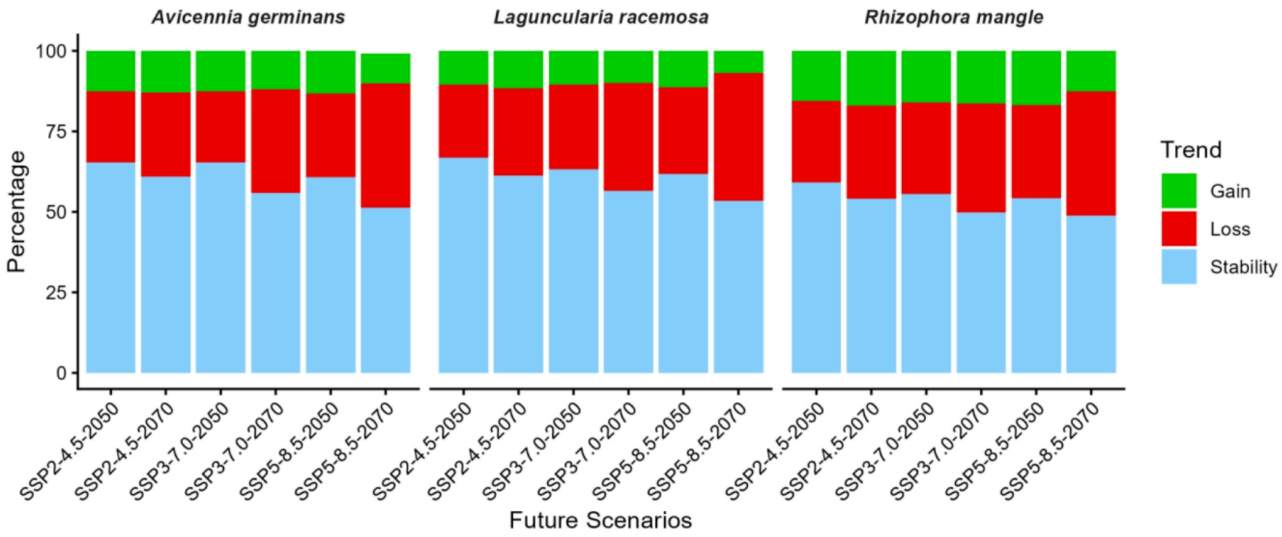

Figure 3

Regional trends in the future potential distribution of *A. germinans, L. racemosa*, and *R. mangle*under six climate change scenarios in the Eastern Pacific. Blue, red, and green bars indicate stability, loss, and gain, respectively.

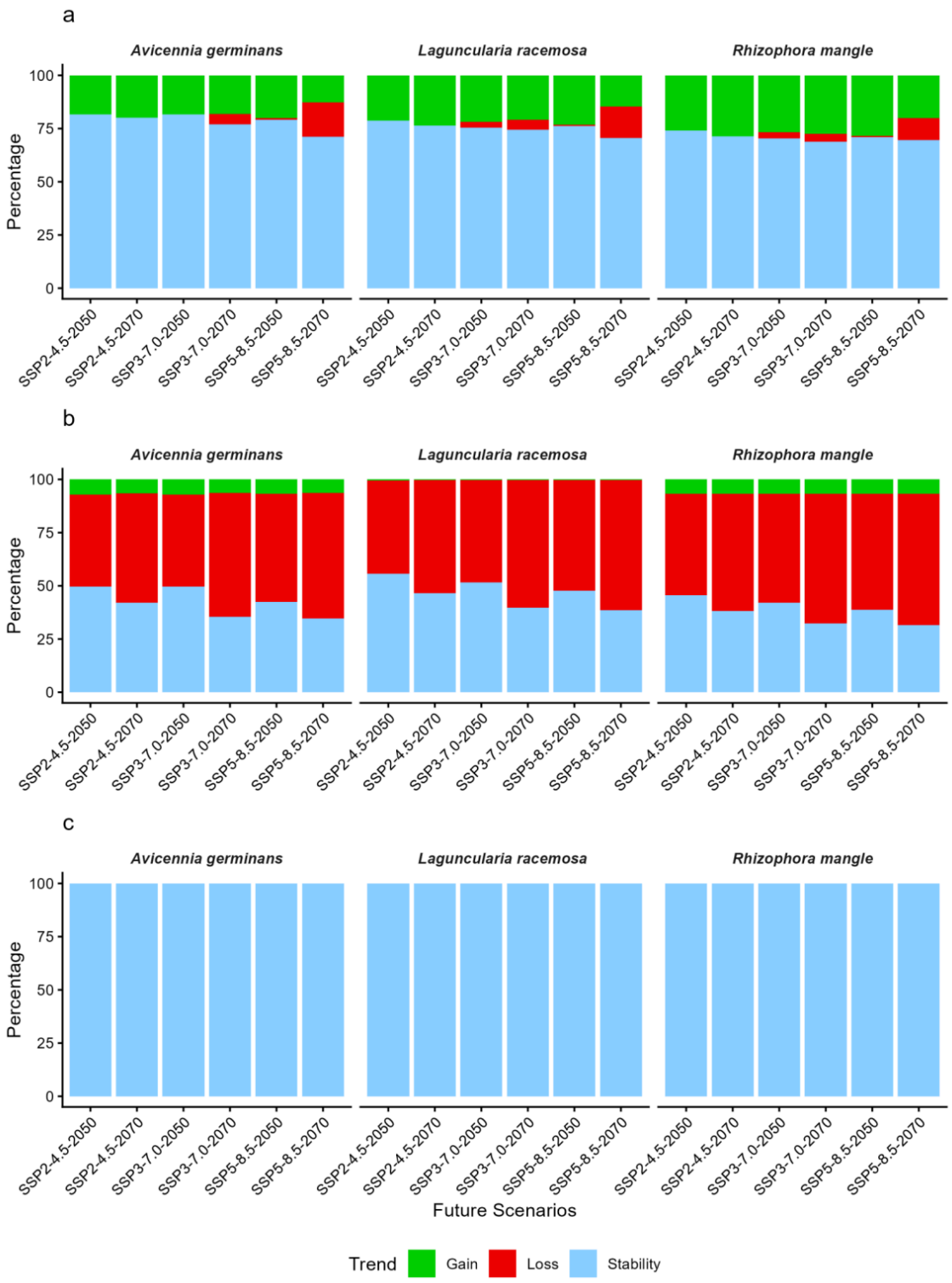

Figure 4

Provincial trends in the future potential distribution of *A. germinans*, *L. racemosa*, and *R. mangle* under six climate change scenarios in the Eastern Pacific. Panels represent the (a) Warm Temperate Northeast Pacific, (b) Tropical Eastern Pacific, and (c) Galápagos provinces. Blue, red, and green bars indicate stability, loss, and gain, respectively.

Supplementary Files

This is a list of supplementary files associated with this preprint. Click to download.

- SupplementaryGonzalezZamorano09June2026.docx
- Table1.docx